# Experimental Study of Excited $^4$H, $^4$He, and $^4$Li Nuclear Systems*

NELSON JARMIE, RICHARD H. STOKES, GERALD G. OHLSEN, AND R. W. NEWSOME, JR.†
*Los Alamos Scientific Laboratory, University of California, Los Alamos, New Mexico*
(Received 15 May 1967)

$^4$He, $^4$Li, and $^4$H have been produced as residual nuclear systems in various reactions induced by deuterons, tritons, and $^3$He ions bombarding deuterium, tritium, and $^3$He targets. The bombarding energy was varied from 12 to 22 MeV, and proton and deuteron spectra were measured at angles from 10° to 35°. The first excited state of $^4$He was seen in the $^3$He$(d,p)^4$He* reaction at an excitation of 20.08±0.04 MeV with a center-of-mass width of 0.43±0.05 MeV. It was also observed in the $^3$He$(t,d)^4$He* reaction at an excitation of 20.00±0.04 MeV with a c.m. width of 0.36±0.05 MeV. There was weak evidence for a second excited state at about 1.2 MeV above the $t+p$ mass. Upper limits on cross sections were set for possible bound states. No direct evidence for unbound states in the $^4$Li or $^4$H systems was observed. Both the continuous spectra and the spectral peaks are discussed and are compared with previous experimental results. Absolute cross sections were measured and are presented.

## INTRODUCTION

MANY aspects of very light nuclei are still not well understood. In some cases shell-model, collective-model, or supermultiplet calculations appear to give an acceptable description, although the choice of appropriate model is not always evident. Descriptions which directly use the nucleon-nucleon interaction have not been extensively developed. One case of particular importance is the highly symmetrical $^4$He nucleus, which has become interesting especially since the discovery of its first excited state. Much theoretical and experimental work has been done recently searching for and studying the energy-level structure of $^4$He and its isobaric neighbors $^4$Li and $^4$H. These nuclei have been studied as compound and residual systems in various scattering and reaction experiments with nucleons, nuclei, pions, and $\gamma$ rays. A guide to the rather extensive experimental and theoretical literature may be found in the following recent articles and the references they contain: for $^4$H, Ref. 1; for $^4$He, Refs. 2–6; and for $^4$Li, Refs. 7–9. A compilation of information on the energy levels of 4-nucleon systems is being prepared by Meyerhof and Tombrello.[10]

At present an excited level of $^4$He at about 20 MeV in excitation is the only well-verified state. Evidence for levels near 21 MeV and higher has been seen, but there is no firm consensus concerning their position and nature. There is also no evidence for a bound or a narrow unbound state in $^4$Li or $^4$H.

This paper describes the results of studying the following reactions at various bombarding energies from about 12 to 22 MeV: $^3$He$(d,p)^4$He, D$(^3$He$,p)^4$He, $^3$He$(t,d)^4$He, $^3$He$(^3$He$,d)^4$Li, T$(d,p)^4$H, T$(t,d)^4$H and D$(t,p)^4$H. The writing of the residual nuclear systems as $^4$He, $^4$H, and $^4$Li in this paper does not necessarily imply the creation of a distinct single nucleus, but is often meant to include the unbound and multibody breakup modes possible. The spectra of the protons and deuterons emitted were measured at various laboratory angles in the range of 10° to 35°. A preliminary report of this work has been published.[11] The $^3$He$(d,p)$ and D$(^3$He$,p)$ reactions have been studied also by Young and Ohlsen,[12] Parker *et al.*,[13] and Zurmühle.[14]

## EXPERIMENTAL METHOD

### General

Gaseous targets contained by thin foils were bombarded with beams from the multiple electrostatic-accelerator system at the Los Alamos Scientific Laboratory. Particles emitted from the nuclear reactions were detected by a $\Delta E$-$E$ semiconductor counter particle-identification system, and the resulting energy spectra were analyzed by a multichannel analyzer.

Deuteron, triton, or $^3$He beams were tightly collimated and allowed to enter a 20-in. scattering chamber. The $^3$He beams were from 10–30 nanoA. The $d$ and $t$ beams varied from 20 to 1000 nanoA, depending on the background problem and high-counting-rate effects in the electronics. The error in the determination of the energy of the beam and the energy spread in the beam were negligible. The gas target was 3.8 cm in diameter, and used 12- or 25-$\mu$ beryllium entrance and exit foils. The composition of the target gases was measured and a purity of better than 99% was found except for the tritium gas, which was found to have a purity of

* Work performed under the auspices of the U. S. Atomic Energy Commission.
† Present address: Bellcomm, Inc., Washington, D. C.
[1] T. A. Tombrello, Phys. Rev. **143**, 772 (1966).
[2] L. E. Williams, Phys. Rev. **144**, 815 (1966).
[3] W. E. Meyerhof, Rev. Mod. Phys. **37**, 512 (1965); W. E. Meyerhof and J. N. McElearney, Nucl. Phys. **74**, 533 (1965).
[4] J. Cerny, C. Détraz, and R. H. Pehl, Phys. Rev. Letters **15**, 300 (1965).
[5] B. R. Barrett, J. D. Walecka, and W. E. Meyerhof, Phys. Letters **22**, 450 (1966).
[6] P. Kramer and M. Moshinsky, Phys. Letters **23**, 574 (1966).
[7] T. A. Tombrello, Phys. Rev. **138**, B40 (1965).
[8] G. J. Igo and W. T. Leland, Phys. Rev. **154**, 950 (1967).
[9] R. G. Kerr, Phys. Rev. **148**, 998 (1966).
[10] W. E. Meyerhof and T. A. Tombrello, Nucl. Phys. (to be published).
[11] G. G. Ohlsen, R. W. Newsome, Jr., and R. H. Stokes, Bull. Am. Phys. Soc. **11**, 9 (1966); R. H. Stokes, Nelson Jarmie, R. W. Newsome, Jr., and G. G. Ohlsen, *ibid.* **11**, 9 (1966).
[12] P. G. Young and G. G. Ohlsen, Phys. Letters **8**, 124 (1964); **11**, 192(E) (1964).
[13] P. D. Parker *et al.*, Phys. Rev. Letters **14**, 15 (1965).
[14] R. W. Zurmühle, Nucl. Phys. **72**, 225 (1965).

(93±1)%. The purity was determined by mass-spectrographic analysis, except for tritium, for which scattering analysis was used. The bulk of the tritium contaminant was hydrogen. The detector collimators were made of tantalum and the geometry used typically resulted in an angular acceptance width of ±0.4°. It was determined that the absolute error in the value of the central angle of the detector system was <0.2°.

The energy resolution in the range of interest was measured by means of the sharp peaks of contaminant reactions and had a value (full width at half maximum) of 120 keV. This number agrees with calculations of geometric energy spreads, energy straggling in the foils, and other effects. The absolute accuracy of the energy scale calibrated as described below, and the linearity of the energy scale were good to ±60 keV.

Corrections in the absolute values of the cross section were made for calibrations of the target pressure gauge and beam-current integrator, for dead time in the pulse-height analyzer and other electronic effects, and for target gas purity. The absolute error (standard deviation) of the cross-section scales was determined to be 12% and was in agreement with the fluctuations of similar runs taken at different times and under different conditions. The relative error in a given spectrum was determined by the counting statistics and was usually 2 to 3% unless otherwise noted.

The charged particles were detected in a semiconductor transmission detector followed by a semiconductor $E$ detector in which the particles were stopped. The $E$ detector was a Li-drifted counter either 2 or 3 mm in depth. The $\Delta E$ detectors were surface-barrier units ranging in thickness from 50 to 350 $\mu$ and were either oriented or were tilted 15° to avoid the effects of channeling. Pulses from the $E$ and $\Delta E$ detectors were used with an analog computer system to distinguish one particle species from all others. To facilitate selection of the desired particle a display was generated on a storage oscilloscope. For each $E-\Delta E$ pulse pair a spot was formed on the storage-tube screen. The vertical displacement of the spot was proportional to $E+\Delta E$ and the horizontal displacement was proportional to $(E+E_0+k\Delta E)\Delta E$, which is the quantity generated by the analog computer to be proportional to the mass. Selection of the appropriate mass and charge group could be made by using the display as a basis for adjusting discriminators. Energy spectra were obtained for the selected particle species by recording the $E+\Delta E$ pulse heights in a gated 400-channel analyzer.

## EXPERIMENTAL PROCEDURE

The chamber and collimators were aligned by optical methods and by obtaining traces of the beam on photographic print paper. The position corresponding to zero angle was determined by requiring that the elastic-scattering intensity be the same for equal positive and negative scattering angles. Gains in the $E$ and $\Delta E$ systems were then equalized, so that the sum $E+\Delta E$ would properly represent the detected-particle energy. The settings on the mass identifier were then adjusted and other electronic alignments and tests were made. The output of the 400-channel analyzer was printed and punched on paper tape for later computer analysis. For each run an energy calibration was performed by detecting groups of the particle of interest at various energies from known reactions, usually elastic scattering. Target-empty background runs were taken to correspond to each data run. A variety of special runs were made with possible contaminant gases such as $H_2$, $CO_2$, air, and $^4$He. Lengthy studies were performed to determine possible idiosyncrasies of the system with respect to counting rate and other parameters.

Representative examples of the raw data are shown in Figs. 1–6. Backgrounds have not yet been subtracted from the data displayed in these figures. The vertical bars represent the error (standard deviation) due to counting statistics. The $E_x$ scales shown in Figs. 1, 3, 4, and 5 are examples of the excitation energy in the residual system ($^4$He, etc.) above the three-body break-up threshold. These scales will be useful in the discussion of the results. The $^3$He$(d,p)$ reaction shown in Fig. 1 had the most interference from contaminant and spurious peaks. Peaks *a*, *b*, and *c* were found to be spurious counting-rate dependent peaks, most likely resulting from the effect of the very intense deuteron elastic-scattering peak on the mass-identifier circuits. The relative magnitudes of these peaks were sensitive to the counting rate in a very nonlinear way, and could be eliminated by running with low beam intensities. Peak *d* resulted from elastic scattering from contaminant hydrogen in the target gas, H$(d,p)$D. This peak was not rate sensitive, but would change in relative height from run to run as the contaminant hydrogen fraction changed. Peak *e* and curve *g* are data from the $^3$He$(d,p)$ reaction, the spectrum cutting off in about channel 25, where the lower-energy protons ceased depositing enough energy in the $E$-counter and the required $E$-$\Delta E$ coincidence was not met. A biased amplifier system was used, so this lower-level cutoff was in an arbitrary channel. Curve *f* shows the empty target background.

Where not obscured by contaminant or spurious peaks, the lack of yield in the upper part of the spectrum is useful for setting upper limits on bound states (in this case, $^4$He). Of note in the 11.75-MeV curve is the structure at about channel 90. This "break" in the curve showed in most of the $^3$He$(d,p)$ data. In this case it is distinct; in several of the cases it was statistically marginal. This "break" was not rate- or run-sensitive, and could not be ascribed to any contaminant. Of special concern was the possibility that contaminant $^4$He in the $^3$He gas might enable the $^4$He$(d,p)^5$He reaction to produce a spurious proton group. This group would lie in the neighborhood of the "break" found in the data. However, careful experimental and theoretical tests

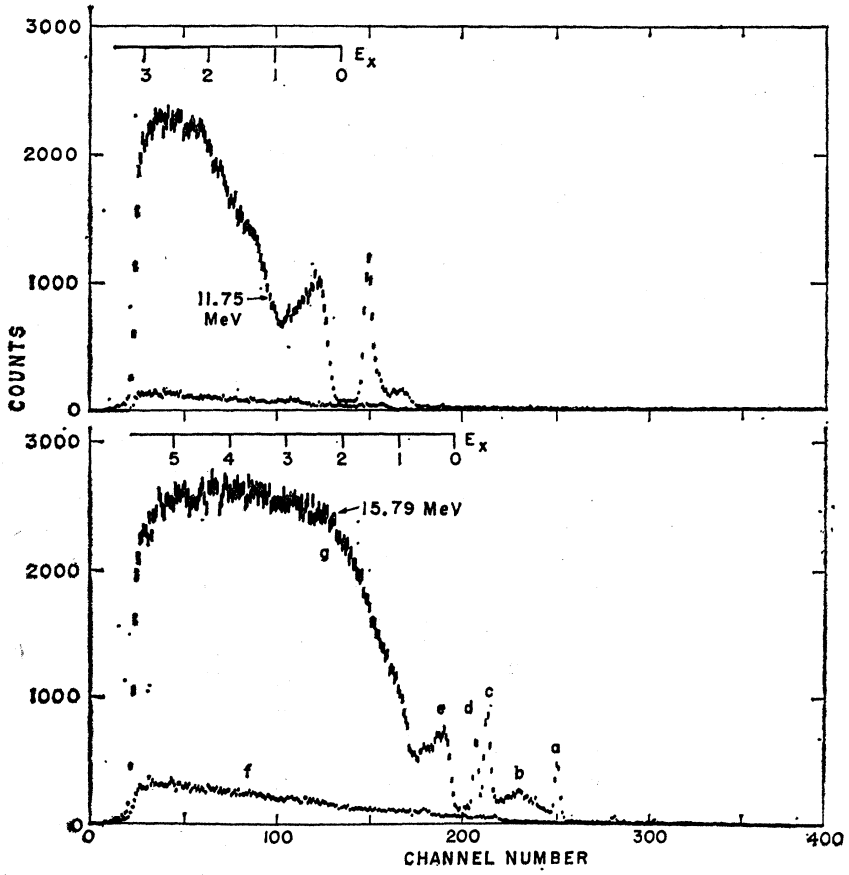


FIG. 1. Typical raw-data spectra for the $^3$He($d,p$) reaction. The 11.75-MeV-bombarding-energy case is at 15° laboratory angle and the 15.79-MeV spectrum is at 10° laboratory angle. The vertical bars indicate statistical errors. The lower series of points is the empty target background. Further details are given in the text.

showed that: (1) Such spurious proton groups would not lie at the same energies as the "breaks"; (2) there was not enough $^4$He in the $^3$He gas to produce an effect; and (3) the width of such groups, because of the width of the $^5$He states, would not be compatible with the data.

Figure 2, an example of the D($^3$He,$p$) reaction, shows larger statistical errors due to the low intensity of $^3$He beams available. In Fig. 3, the $^3$He($t,d$) reaction, the spectrum is typical of the contaminant-free data obtained when deuterons were detected. The T($d,p$) data in Fig. 4 is similar to $^3$He($d,p$) in Fig. 1 except that the H($d,p$)D peak at about channel 225 is much larger because the amount of hydrogen contaminant in the target gas has increased. In Fig. 5, part of the data spectrum is obscured by the peak at channel 125 which is due to the H($t,d$)D reaction. In Fig. 6, an example of a D($t,p$)$^4$H spectrum, all the structure past channel 170 is rate-sensitive and spurious, except for the peak at channel 185, which is due to the H($t,p$)T reaction.

## RESULTS

To present the data in the clearest fashion, the raw data has been considerably edited. The results are shown in Figs. 7 through 20. Backgrounds have been subtracted, energy calibrations made, and the various cross-section factors have been included so that the curves may be presented in terms of differential cross section versus particle energy. Smooth curves have been drawn including any structure judged to be statistically significant. These curves have been terminated at a particle energy about 0.75 MeV higher than the detector cutoff energy to avoid systematic errors in the lower-energy parts of the spectra. Spurious and contaminant peaks have been left out; the regions where they have obscured the data have been left dashed or blank. The arrows on the top edge of the graphs indicate the kinematic threshold for three-body breakup. Except for Fig. 10, all curves in Figs. 7 through 20 show energies and cross sections in the laboratory system. In Fig. 10 the cross section is in the c.m. system. The value of the maximum excitation of the residual mass-4 system studied in each reaction will be given. This value, together with the range of the upper limits on bound states and the sample excitation energy scales shown in Figs. 1, 3, 4, and 5, can be used to indicate the range of excitation studied in each case. To aid the reader in the interpretation of the curves, formulas to calculate the excitation energy of the residual system are given in Appendix I.

## REDUCTION OF RESULTS AND PRELIMINARY DISCUSSION

### 1. $^3$He($d,p$) Reaction and States in $^4$He

Relatively sharp peaks in the curves in Figs. 7–9 at a proton energy just below the three-body breakup thresh-

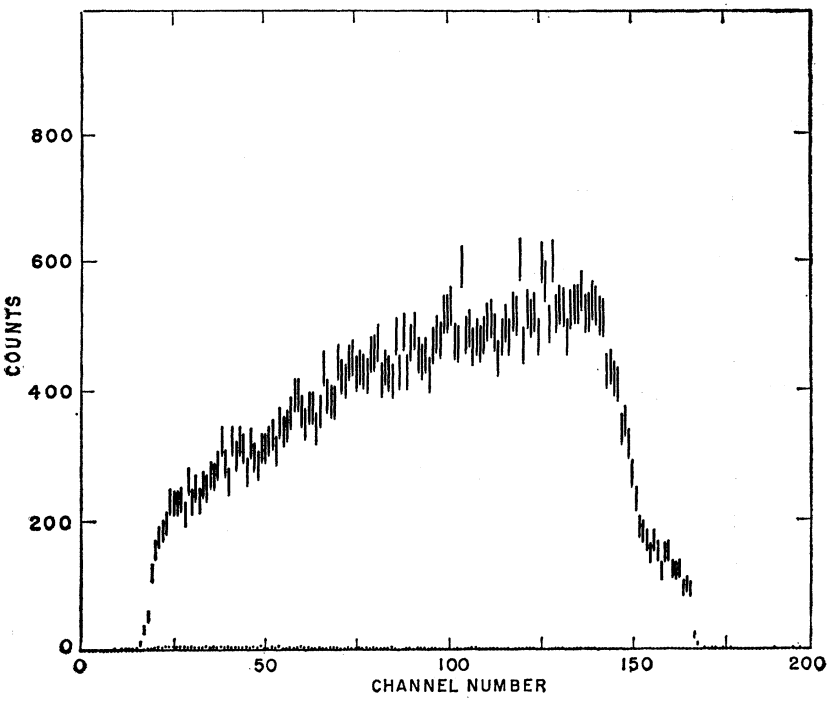


FIG. 2. Raw-data spectrum for the D($^3$He,$p$) reaction. The data are for 21.78-MeV bombarding energy and 10° laboratory angle.

old give a distinct verification of the existence of first excited state of $^4$He, the "20-MeV state." The intensity of this state decreases with higher angle and higher energy until, as shown in Fig. 9, the peak has all but disappeared. If one assumes the other part of the curves falls to the three-body threshold in a simple way and makes a reasonable subtraction, the information in Fig. 20 and Table I is obtained. This simple subtraction neglects interference, and the effects of the reaction mechanisms involved, but within the limits of error stated the results are probably meaningful. A much more detailed analysis[15] would be necessary to extract more accurate parameters. For all the $^3$He($d$,$p$) curves, a combined value for the excitation in $^4$He is (0.27±0.04) MeV above the $t+p$ threshold, or (20.08±0.04) MeV above the ground state. The laboratory width of the subtracted "20-MeV state" is (0.52±0.05) MeV, which, when unfolded from the experimental resolution and transformed to the $t+p$ c.m. system, gives a width of (0.43±0.05)MeV. These results will be further discussed below. The areas of the peaks may be measured to obtain the cross section for the $^3$He($d$,$p$) reaction which leads to the first excited state. The results are shown in Fig. 10. Transformation to the c.m. system is possible because variations in the c.m. angle and the transformation Jacobian are small over the region of interest. The errors shown are relative standard deviations. The absolute error in the cross-section scale is 12%.

At a proton energy roughly 1 MeV lower in energy than the "20-MeV" state peak in most of the curves is a small bump or break in the slope of the spectrum which we shall call a "break." The approximate excitation energies which correspond to these "breaks" are shown in Table I. Assuming these effects stem from some single phenomenon in $^4$He, one calculates an average excitation above the $t+p$ threshold of (1.16±0.07)MeV. It should be noted that the statistical distribution of the individual values about the average does not appear to follow a normal distribution. The stated average corresponds to an excitation in $^4$He of (20.97±0.07)MeV. The right-hand shoulder of the broad plateaus of the spectra in each case are at an excitation energy above the $t+p$ threshold of about 2.2 MeV. The largest range of

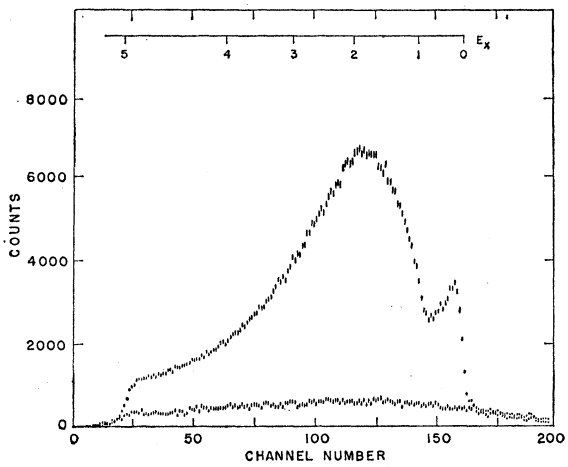


FIG. 3. Typical raw-data spectrum for the $^3$He($t$,$d$) reaction. The data are for 21.8-MeV bombarding energy and 10° laboratory angle. See text for details.

[15] D. U. L. Yu and W. E. Meyerhof, Nucl. Phys. 80, 481 (1966).

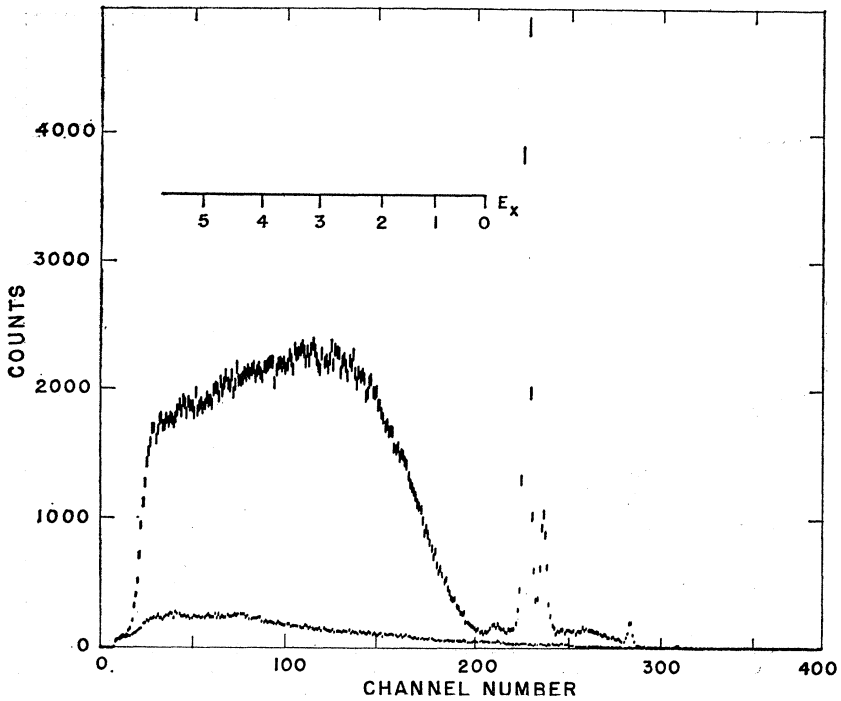


FIG. 4. Typical raw-data spectrum for the T($d$,$p$) reaction. The data are for 19.82-MeV bombarding energy and 10° laboratory angle. See text for details.

excitation in the $^4$He system for this reaction is observed in curve D of Fig. 8, where the lowest proton energy corresponds to 7.6 MeV in excitation energy above the $t+p$ mass. The largest value for Fig. 7 is curve E, with 6.3 MeV.

The lack of yield at higher proton energies gives an upper limit to the cross section for a bound state of $^4$He, of width (c.m.) less than 0.1 MeV and in the range of excitation in $^4$He of 11.0 to 18.3 MeV, of 15 $\mu$b/sr. This limit is calculated from the 10° 11.75-MeV data but is about the same for the 10° and 15° data at all the energies.

### 2. D($^3$He,$p$) Reaction and States in $^4$He

The spectrum in Fig. 11 also shows the "20-MeV" state, but not as distinctly. Analysis of this peak gives the following value for the c.m. differential cross section for the reaction going to the "20-MeV" state of $^4$He: (2.7±0.7)mb/sr at a c.m. angle of 16.8°, where the error is an absolute standard deviation. For purposes of comparison, one may transform this datum into the equivalent $^3$He($d$,$p$)$^4$He* system. In this system the c.m. cross section is, of course, the same, the c.m. angle is 163.3°, the laboratory angle is 151.2°, and the laboratory bombarding energy is 14.5 MeV.

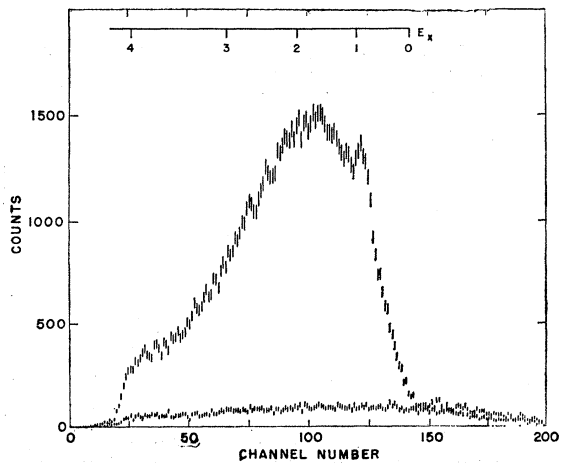


FIG. 5. Typical raw-data spectrum for the T($t$,$d$) reaction. The data are for 21.78-MeV bombarding energy and 12° laboratory angle. See text for details.

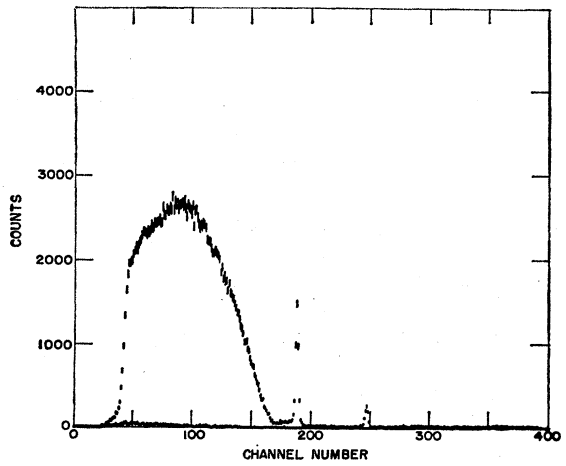


FIG. 6. Typical raw-data spectrum for the D($t$,$p$) reaction. The data are for 17.75-MeV bombarding energy and 15° laboratory angle. See text for details.

TABLE I. Widths and excitations in $^3$He$(d,p)^4$He. $E_0$ is the laboratory bombarding energy, $\Gamma$ the width (FWHM), and $E'$ the excitation energy above the three-body breakup threshold.

| Lab angle (deg) | $E_0$ (MeV) | "20-MeV" state $\Gamma$ (MeV) | "20-MeV" state $E'$ (MeV) | "Break" $E'$ (MeV) |
|---|---|---|---|---|
| 10 | 11.75 | 0.60 | 0.32 | 1.23 |
| 10 | 13.76 | 0.50 | 0.20 | 1.17 |
| 10 | 15.79 | 0.50 | 0.22 | 1.27 |
| 10 | 17.80 | 0.50 | 0.29 | 1.27 |
| 10 | 19.82 | 0.50 | 0.24 | 1.15 |
| 15 | 11.75 | 0.50 | 0.39 | 1.36 |
| 15 | 13.76 | 0.55 | 0.29 | 1.15 |
| 15 | 15.79 | 0.55 | 0.26 | 1.29 |
| 15 | 17.80 | ... | ... | 1.00 |
| 15 | 19.82 | ... | ... | 1.04 |

The broad, main peak may be integrated to give a laboratory cross section for the residual processes (without the "20-MeV" state) of (723±36)mb/sr; the error quoted is the error due to uncertainty in the integration; the absolute standard deviation is 12%. The maximum of the broad main peak is at an excitation energy above the $t+p$ threshold of about 1.5 MeV. The maximum excitation in the $^4$He system observed in this reaction is 6.7 MeV above the $t+p$ mass.

The lack of yield at high proton energies enables one to calculate an upper limit to the cross section for a bound state of $^4$He, of width (c.m.) less than 0.1 MeV and in the range of excitation in $^4$He from 17.0 MeV to the $t+p$ breakup threshold, of 10 $\mu$b/sr.

### 3. $^3$He$(t,d)$ Reaction and States in $^4$He

Figures 12 and 13 also show distinct peaks due to the first excited "20-MeV" state of $^4$He; indeed, curve C

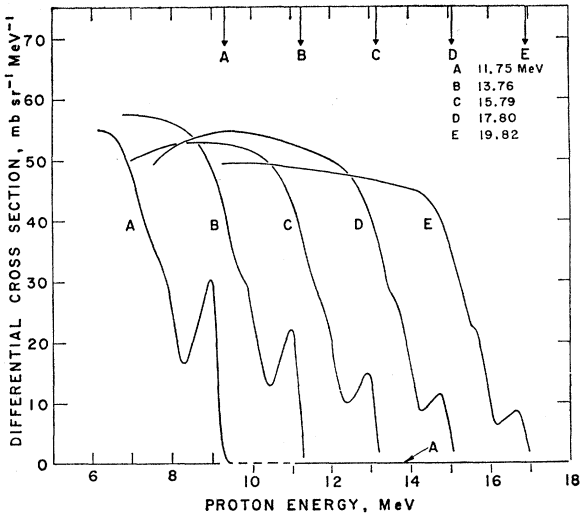


FIG. 7. Experimental results for the $^3$He$(d,p)$ reaction at 10° laboratory angle. Shown are the bombarding energies. The upper arrows indicate the kinematic threshold for three-body breakup. For each curve, the cross section for proton energies above the threshold is zero, shown in curve A as an example. The dashed section is a region obscured by a contaminant reaction.

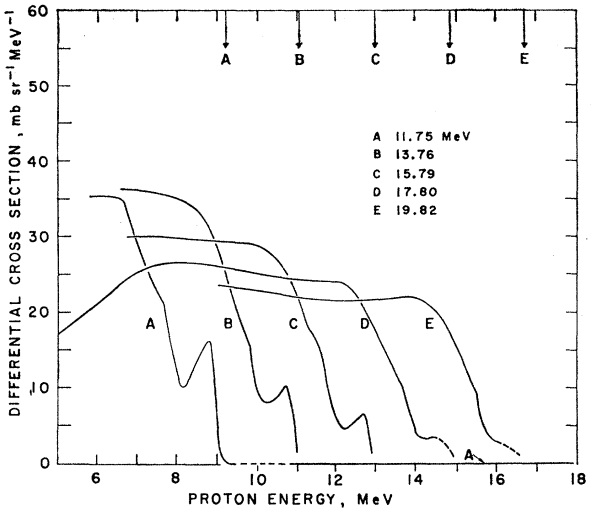


FIG. 8. Experimental results for the $^3$He$(d,p)$ reaction at 15° laboratory angle. Shown are the bombarding energies.

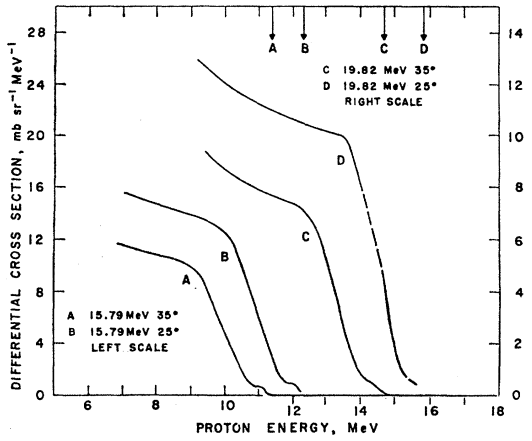


FIG. 9. Experimental results for the $^3$He$(d,p)$ reaction for the bombarding energies and laboratory angles shown.

of Fig. 12 shows the most striking resonance shape ascribable to the first excited state of $^4$He that has been published. The excitation of the peak in the $^4$He system in each case was about 0.18 MeV above the $t+p$ threshold; more precisely, an average excitation above

TABLE II. Differential cross sections from integration of $^3$He$(t,d)^4$He spectra. $E_0$ is the laboratory bombarding energy. Where two errors are shown, they are the relative and absolute standard deviations, respectively. One error alone is the absolute error.

| $E_0$ (MeV) | Lab angle (deg) | Broad peak $\sigma(\theta)$ (lab) (mb/sr) | "20-MeV" state $\sigma(\theta)$ (lab) (mb/sr) | "20-MeV" state $\sigma(\Omega)$ (c.m.) (mb/sr) |
|---|---|---|---|---|
| 17.75 | 10 | 156±5±8 | 20.6±2.0 | 4.5 ±0.4 |
| 17.75 | 12 | 82±3±4 | 7.1±0.9 | 1.6 ±0.2 |
| 17.75 | 15 | 56±3±4 | 2.2±0.3 | 0.49±0.07 |
| 21.78 | 10 | 188±6±12 | 11.6±1.0 | 2.9 ±0.2 |
| 21.78 | 15 | 149±6±12 | 1.8±0.4 | 0.46±0.1 |
| 21.78 | 20 | 81±6±12 | ≤0.6 | ≤0.16 |

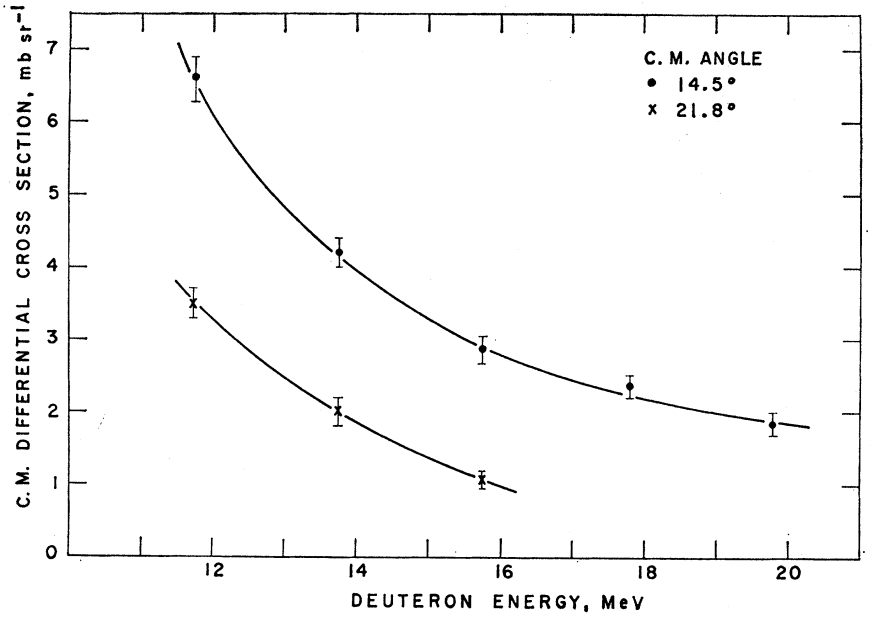


FIG. 10. Excitation function for the production of the first ("20-MeV") excited state of $^4$He by the reaction $^3$He$(d,p)^4$He*. The 14.5° curve comes from the 10°-laboratory-angle data and the 21.8° curve from the 15°-laboratory-angle data. The deuteron energies are laboratory bombarding energies.

the $t+p$ threshold of (0.18±0.04)MeV for the "20 MeV" state was obtained from this data. This corresponds to an excitation in $^4$He of (20.00±0.04)MeV. The laboratory full widths at half maximum in the 10° and 12° data (Fig. 12) give an average width of the peak of (0.55±0.07)MeV. When unfolded from the experimental resolution and transformed to the $^4$He system the value of the width (FWHM) is (0.36±0.05)MeV.

The areas of the "20-MeV" state peaks and of the spectra minus this state were measured as previously described and the results are given in Table II. The approximate c.m. angles of the "20-MeV" state for the 17.75- and 21.78-MeV data are 21.8° and 20.2°, respectively. Corresponding to the "breaks" of the $^3$He$(d,p)$ data, there do exist curious distortions in the$^3$ He$(t,d)$ data. The right-hand edge of the flat top of curve B, Fig. 12, the bulges on the right side of the broad peak of curve C in both Figs. 12 and 13, and the rather indistinct strange shape on the right-hand sides of the broad peak of curves A and B of Fig. 13 all correspond to about 1.2-MeV excitation in $^4$He above the $t+p$ breakup threshold and may thus be related to the "breaks" of the $^3$He$(d,p)$ data. The left-hand edge of the flat top of curve B, Fig. 12, and the broad main peaks of Fig. 13 all correspond to energies of excitation of $^4$He above the $t+p$ mass of about 1.8 MeV. The largest range of

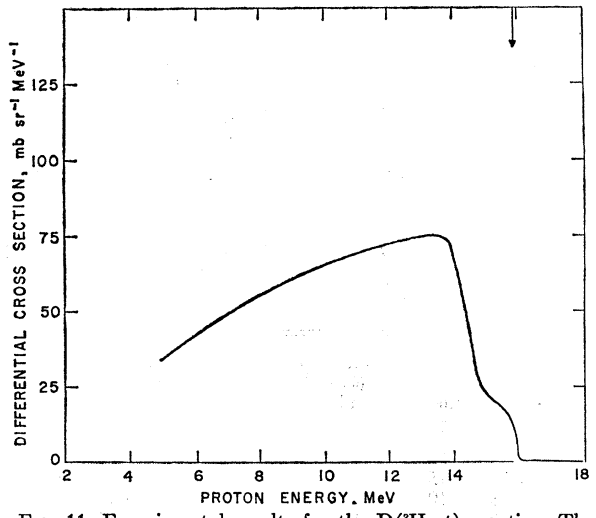


FIG. 11. Experimental results for the D($^3$He,$p$) reaction. The data are for 21.78-MeV bombarding energy and 10° laboratory angle. The relative error of this data is ±10%.

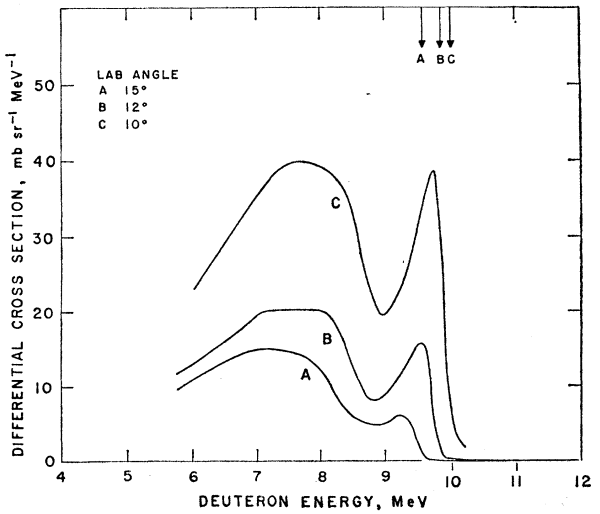


FIG. 12. Experimental results for the $^3$He$(t,d)$ reaction at 17.75-MeV bombarding energy and the laboratory angles shown.

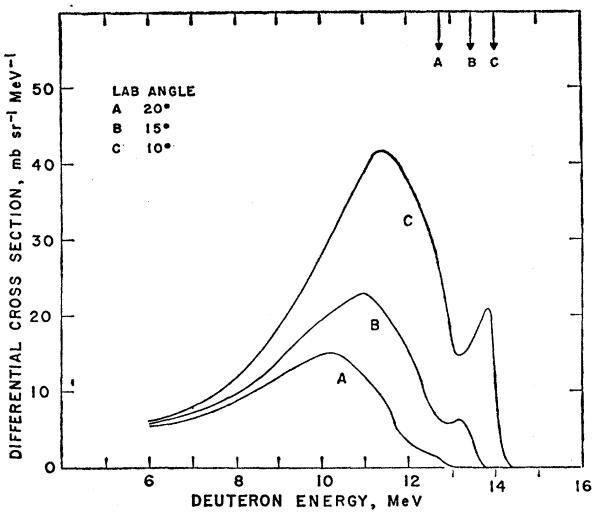


FIG. 13. Experimental results for the $^3$He($t$,$d$) reaction at 21.8-MeV bombarding energy and the laboratory angles shown.

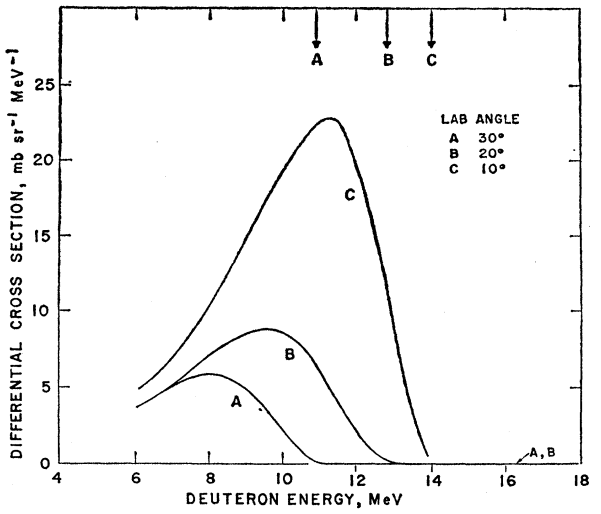


FIG. 14. Experimental results for the $^3$He($^3$He,$d$) reaction at 21.78-MeV and the laboratory angles shown.

excitation in the $^4$He system for this reaction is observed in curve C of Fig. 13, where the lowest deuteron energy corresponds to 4.7 MeV in excitation energy above the $t+p$ mass. The largest value for Fig. 12 is curve B, with 2.4 MeV.

The lack of yield above the $t+p$ threshold gives an upper limit for the cross section of a bound state of $^4$He, of width (c.m.) less than 0.1 MeV and in the range of excitation in $^4$He, from 6.7 MeV to the $t+p$ mass, of 10 $\mu$b/sr. This informaton is extracted from the 17.75-MeV data.

### 4. $^3$He($^3$He,$d$) and States in $^4$Li

In Fig. 14 it may be seen that no peak exists that corresponds to the $^4$He "20-MeV" state in the previous reactions. Here also no distortions corresponding to the "breaks" seem to be eivdent. The single broad peak in evidence has its peak at an excitation in the "$^4$Li" system of about 2.0 MeV above the $p+^3$He breakup threshold. The laboratory cross sections resulting from the integration of these spectra are given in Table III. From the lack of yield at higher deuteron energies, an upper limit is found for the cross section, yielding a bound state of $^4$Li, of width (c.m.) less than 0.1 MeV, of 10 $\mu$b/sr for a mass range of $^4$Li from the $p+^3$He mass to 3.8 MeV less than the $p+^3$He mass, and 40 $\mu$b/sr down to 8.2 MeV less than the $p+^3$He mass. The largest range of excitation in the $^4$Li system for this reaction is observed in curve C (Fig. 14), where the lowest deuteron

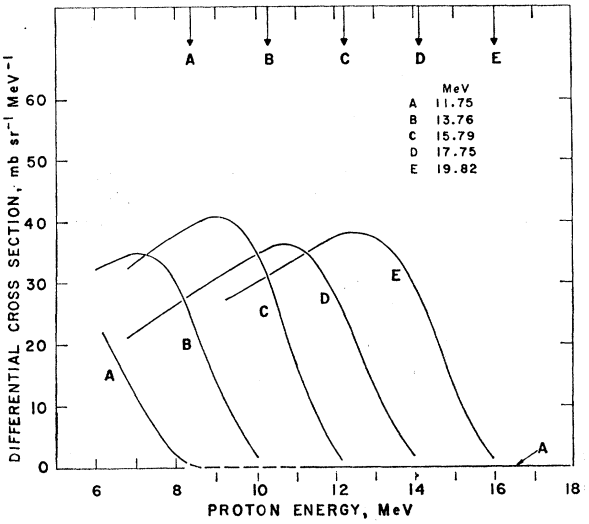


FIG. 15. Experimental results for the T($d$,$p$) reaction at a laboratory angle of 10° and the bombarding energies shown.

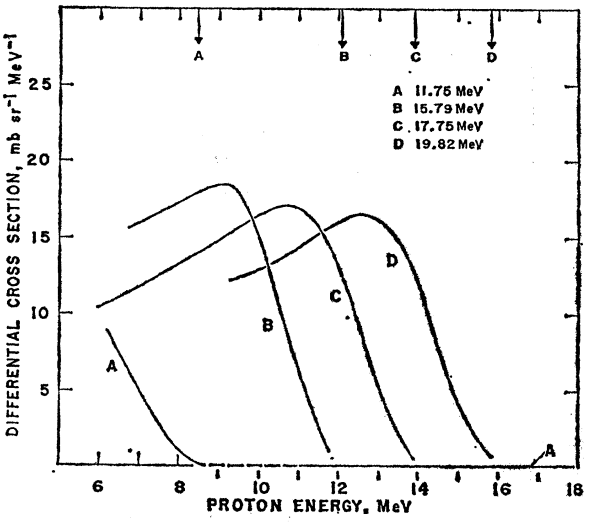


FIG. 16. Experimental results for the T($d$,$p$) reaction at a laboratory angle of 15° and the bombarding energies shown. The data expected at 13.76 MeV was lost because of equipment failure.

TABLE III. Laboratory differential cross sections for the $^3$He($^3$He,$d$) reaction at 21.78-MeV bombarding energy. The error shown is the absolute standard deviation. The relative error is the same.

| Lab angle (deg) | $\sigma(\theta)$ (mb/sr) |
|---|---|
| 10 | 112.4±5.5 |
| 20 | 44.7±4.4 |
| 30 | 24.4±4.8 |

energy corresponds to 4.75-MeV excitation energy above the $p$+$^3$He mass.

### 5. T($d$,$p$), D($t$,$p$) Reactions, and States in $^4$H

Figures 15–17 show proton spectra from the T($d$,$p$) reaction. Again, no peak or structure corresponding to the "20-MeV state" in $^4$He is indicated for the residual $^4$H system. The excitation energy in the $n$+T system for the broad peaks in the 10° and 15° data are in every case about 2.3 to 2.5 MeV. It is interesting to note that at a given angle the maximum cross section is roughly constant. Also, no "break" or other indistinct structure as seen in the $^3$He($d$,$p$) data appears here. The largest range of excitation in the $^4$H system is observed in curve C of Fig. 16, where the lowest proton energy corresponds to 6.3 MeV in excitation energy above the $n$+$t$ mass. The largest value for Fig. 15 is curve D with 5.8 MeV.

The lack of yield at proton energies above the kinematic threshold for 3-body breakup gives an upper limit to the cross section for a bound state of $^4$H, of width (c.m.) less than 0.1 MeV, of 10 $\mu$b/sr for the mass range of 2.2 to 8.8-MeV excitation energy below the $n$+T mass. This best value for this limit comes primarily from the 11.75-MeV data.

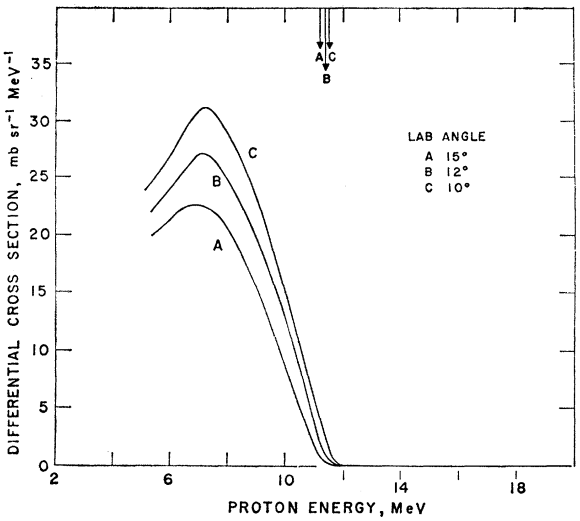


FIG. 18. Experimental results for the D($t$,$p$) reaction at a bombarding energy of 17.75-MeV and the laboratory angles shown.

Figure 18 shows data on the inverse reaction, D($t$,$p$). The broad peaks are at an excitation of about 2.8 MeV in the $n$+T system. The maximum excitation observed in the $^4$H system in the D($t$,$p$) reaction is about 3.8 MeV above the $n$+$t$ mass for each curve in Fig. 18. As is the $T(d,p)$ reaction, no sharp states are seen. The equivalent laboratory bombarding energy, as if the reaction were observed in the T($d$,$p$) system with a triton at rest, is 11.8 MeV, and the equivalent T($d$,$p$) laboratory angles are in the region of 135°. The lack of yield above the kinematic threshold gives an upper limit to the cross section for a bound state of $^4$H, of width (c.m.) less than 0.1 MeV, of 10 $\mu$b/sr for the mass range of from 1.1- to 10.9-MeV excitation energy below the $n$+$t$ mass.

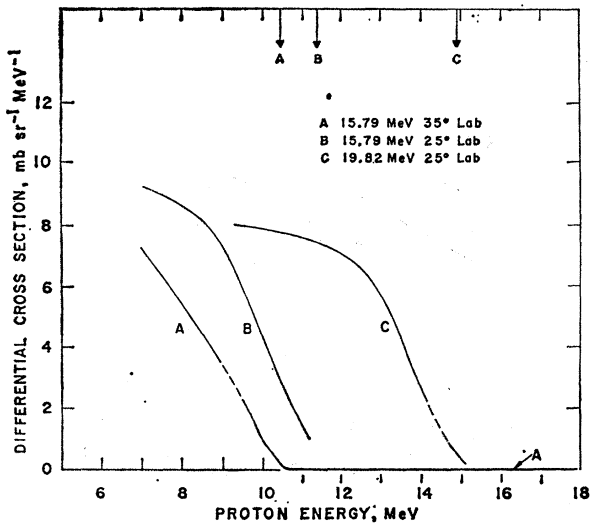


FIG. 17. Experimental results for the T($d$,$p$) reaction at the bombarding energies and laboratory angles shown.

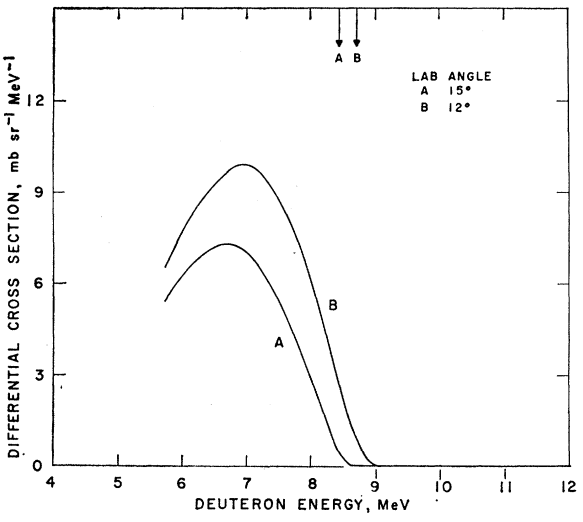


FIG. 19. Experimental results for the $T(t,d)$ reaction at 17.75-MeV bombarding energy and the laboratory angles shown.

### 6. T($t$,$d$) Reaction and States in $^4$H

Figures 19 and 20 show a simple broad peak without the additional structure seen in the $^3$He($t$,$d$) reactions. The broad peaks in the 17.75-MeV data are at roughly 1.1-MeV excitation in the $n$+T system and in the 21.78-MeV data are each about 1.7 MeV in excitation. The spectra may be integrated to give laboratory differential cross sections, and the results are shown in Table IV. The largest range of excitation in the $^4$H

TABLE IV. Laboratory differential cross sections for the T($t$,$d$) reaction. See the caption of Table II for definitions.

| $E_0$ (MeV) | Lab angle (deg) | $\sigma(\theta)$ (mb/sr) |
|---|---|---|
| 17.75 | 12 | 30.5±3.0± 6.6 |
| 17.75 | 15 | 21.7±2.2± 6.3 |
| 21.78 | 10 | 136.8±4.1±16.5 |
| 21.78 | 12 | 107.9±3.2±14.2 |
| 21.78 | 15 | 83.6±2.5±10.5 |
| 21.78 | 20 | 57.1±1.7± 8.1 |

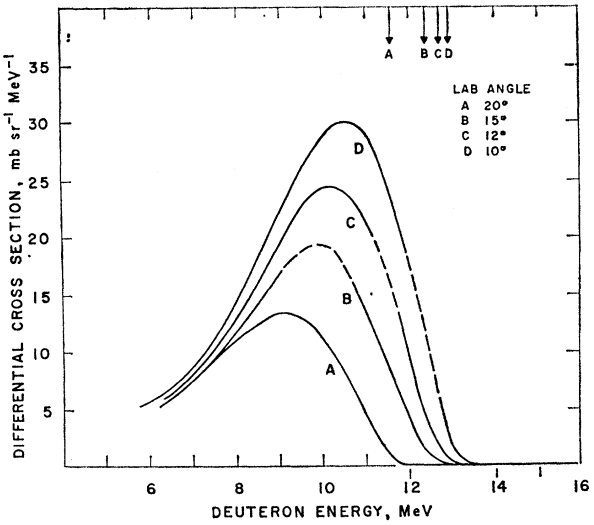


FIG. 20. Experimental results for the T($t$,$d$) reaction at 21.78-MeV and the laboratory angles shown.

system for this reaction is observed in curve D of Fig. 20, where the lowest deuteron energy corresponds to 4.04 MeV above the $n$+$t$ mass. The largest value for Fig. 19 is for curve B, with 1.7 MeV. The lack of yield above the breakup threshold gives an upper limit to the cross section for a bound state of $^4$H, of width (c.m.) less than 0.1 MeV, of about 10 $\mu$b/sr. This upper limit is valid for a range of mass relative to the $n$+T mass of 0 to −12.8 MeV, except for a small region near −5.6 MeV which was obscured by a contaminant reaction.

## FURTHER DISCUSSION AND CONCLUSIONS

### 1. Bound States

As has been indicated in the previous section, evidence for a level in $^4$H, $^4$He, and $^4$Li stable against particle decay was not observed over broad ranges of excitation. In particular, a state in $^4$He at (14.8±1.9)-MeV predicted by Bartis[16] was not observed. Bartis introduces a model for $A=4n$ self-conjugate nuclei in which there is a strong pairing correlation and successfully accounts for the first-excited $0^+$ states of $^{12}$C and $^{16}$O. In the present experiment a level in $^4$He 1% as strong as the "20-MeV" state would easily have been observed. Possibly the state predicted by Bartis, a system of contra-rotating nuclear pairs, may be only weakly excited by the configurations of target and projectile in our experiment.

### 2. Unbound States and Broad Spectral Peaks

A spectral peak corresponding to the "20-MeV" state in $^4$He is readily observed in both the $^3$He($d$,$p$) and $^3$He($t$,$d$) reactions and falls in intensity with increasing angle of observation and bombarding energy. No corresponding peak is seen in the reactions producing $^4$Li and $^4$H systems, which verifies that the state has $T=0$.

Both the excitation energy and the width of the "20-MeV" state measured in the ($t$,$d$) reaction are slightly smaller than the values from the ($d$,$p$) reaction. The ($t$,$d$) data are probably more reliable since the experimental peaks are sharper and the subtraction of other processes is less ambiguous. Our values for the energy agree with that found by Young and Ohlsen,[12] who also used the $^3$He($d$,$p$)$^4$He reaction. However, the standard deviation of all the values for this energy level measured by the various reactions, including ours, (see the summary in Ref. 4) is about 180 keV—much larger than the individual errors quoted in each experiment. Whether this difference is due to systematic error or a lack of a sufficiently sophisticated interpretation of the mechanisms involved remains to be seen. The situation concerning the measured widths is similar.

The "breaks" and other distortions seen in the $^3$He($d$,$p$) and $^3$He($t$,$d$) data might possibly correspond to the second excited state, presumably $T=0$, seen by Parker *et al.*,[13] and Cerny, Détraz, and Pehl.[4] In our data no similar effects are observed in reactions leading to $^4$H and $^4$Li systems, supporting a $T=0$ assignment. The data indicating these "breaks" are not very distinctive and should be used primarily to motivate clarifying experiments.

The interpretation of the broad spectra, exclusive of the "20-MeV" state peaks and the "breaks" already discussed, is very ambiguous. For example, Cerny, Détraz, and Pehl,[4] observing a similar broad peak in $^6$Li($p$,$t$)$^4$Li, interpret it as a "state" in $^4$Li and extract an excitation energy. Kerr,[9] on the other hand, investigating the $^3$He($d$,$n$) reaction, sees broad peaks which are

[16] F. J. Bartis, Nuovo Cimento **45B**, 113 (1966).

very similar in shape and approximate cross section to our data of the mirror reaction T($d$,$p$). Kerr concludes that his peaks cannot be interpreted as a state in $^4$Li and accounts for his shapes in terms of a simple model of the production of particle pairs in states of nonzero angular momentum. The present authors feel that the interpretation of spectral peaks several MeV in breadth is difficult and that the various reaction mechanisms, phase-space considerations, and other possibly nonresonant phase shifts will greatly influence the spectral shapes obtained. Only when the peak is narrow, can resonance parameters be extracted with any confidence. Indeed, the present disagreement about the energy and width of the "20-MeV" state of $^4$He is probably mostly due to the neglect of the effect of the reaction mechanism involved. An adequate treatment of the broader peaks probably necessitates a more sophisticated approach, for example, analyzing earlier work on spectra from the $^3$H+$d$ and $^3$He+$d$ reactions as was done by Yu and Meyerhof[15]. To fit the data they include details of the reaction mechanisms and known $n$+$^3$He and $p$+$^3$H phase shifts for the effects of the final-state interactions, and conclude that it will be difficult using such reactions to reverse the process and extract nuclear phase shifts concerning the residual system, in this case, $^4$He.

The broad peaks in all the present reactions [except $^3$He($d$,$p$)] and in most similar reactions in other experiments[9,17] rise from threshold and fall at lower energies in much the same fashion, independent of isospin, giving support to the idea that reaction mechanisms and phase-space factors may dominate the shape. The fact that the $^3$He($d$,$p$)$^4$He* spectra do not fall rapidly at low energies can be generally explained by the fact that secondary protons from the breakup of the $^4$He* system are expected to add to the lower-energy yields.

The reaction cross sections generally fall with increasing angle, in agreement with the concept that some kind of direct reaction mechanism is important. The variation of the cross sections with energy is not notable, nor is it expected to be as the excitation in the compound systems is very high. It is interesting to note, however (as in Fig. 7, for example) that the energy variation of the "20-MeV" state peak is qualitatively different than the remaining spectra.

### 3. Final Remarks

It is doubtful that improvements in the knowledge of higher excited states in mass-4 systems is to be gained by the present type of experiment. It is possible that advanced 2-parameter experiments, or experiments with polarized particles, may be useful. Information on the broader states and nonresonant phase shifts is probably better sought by direct scattering experiments, where the system of interest is the compound system.

[17] H. W. Lefevre, R. R. Borchers, and C. H. Poppe, Phys. Rev. **128**, 1328 (1962).

## ACKNOWLEDGMENTS

Discussions with W. E. Meyerhof and D. C. Dodder have been most helpful. The support of R. L. Henkel, R. Woods, and the many other people concerned with the operation of the electrostatic accelerators is gratefully acknowledged.

## APPENDIX

The relationship between the observed (laboratory) energy of a particle and the excitation energy of the residual-particle unstable system is as follows[18]: We denote the observed particle by the subscript 1, the residual interacting particles by 2 and 3, and the projectile and target by the subscripts $p$ and $t$. The relative energy between particles 2 and 3 may then be written

$$E_{2-3}=E^c_{\rm tot}-\frac{m_p+m_t}{m_2+m_3}[E_1{}^l-2a_1(E_1{}^l)^{1/2}\cos\theta_1{}^l+a_1{}^2],$$

where $E_1{}^l$ and $\theta_1{}^l$ are the laboratory energy and angle, respectively. The quantity $a_1$ is given by

$$a_1=(m_1m_pE_p{}^l)^{1/2}/(m_p+m_t).$$

The quantity $E^c_{\rm tot}$, the total energy available in the c.m. system, is given by

$$E^c_{\rm tot}=Q+\frac{m_t}{m_p+m_t}E_p{}^l,$$

where $E_p{}^l$ is the laboratory energy of the projectile. The $Q$ values are those for the three-particle breakup reaction and are tabulated below in Table V.

TABLE V. $Q$ values for the three-body breakup reactions studied.

| Reaction | $Q$ (MeV) |
|---|---|
| $^3$He+$d\rightarrow p+t+p$ | −1.461 |
| $^3$He+$d\rightarrow p+^3$He+$n$ | −2.225 |
| $^3$He+$t\rightarrow d+t+p$ | −5.493 |
| $^3$He+$t\rightarrow d+^3$He+$n$ | −6.257 |
| $t+d\rightarrow p+t+n$ | −2.225 |
| $t+t\rightarrow d+t+n$ | −6.257 |
| $^3$He+$^3$He$\rightarrow d+^3$He+$p$ | −5.493 |

[18] G. G. Ohlsen, Nucl. Instr. Methods **37**, 240 (1965).